Earth Syst. Sci. Data Discuss., 4, 71–97, 2011
www.earth-syst-sci-data-discuss.net/4/71/2011/
doi:10.5194/essdd-4-71-2011

Open Access Earth System Science Data Discussions

Proglacial river dataset from the Akuliarusiarsuup Kuua River northern tributary, Southwest Greenland, 2008–2010

A. K. Rennermalm[1], L. C. Smith[2], V. W. Chu[2], R. R. Forster[3], J. E. Box[4], and B. Hagedorn[5]

[1]Department of Geography, Rutgers, The State University of New Jersey, 54 Joyce Kilmer Avenue, Piscataway, NJ 08854-8045, USA
[2]Department of Geography, University of California, Los Angeles, 1255 Bunche Hall, P.O. Box 951524, Los Angeles, CA 90095-1524, USA
[3]Department of Geography, University of Utah, 260 S. Central Campus Dr., Salt Lake City, UT 84112, USA
[4]Department of Geography, The Ohio State University, 1036 Derby Hall, 154 North Oval Mall, Columbus, OH 43210-1361, USA
[5]Environment and Natural Resources Institute, University of Alaska Anchorage, 3211 Providence Drive, Anchorage, AK 99508, USA

Received: 8 July 2011 – Accepted: 25 July 2011 – Published: 14 September 2011

Correspondence to: A. K. Rennermalm (arennerm@rci.rutgers.edu)

Published by Copernicus Publications.

Abstract

Pressing scientific questions concerning the Greenland ice sheet's climatic sensitivity, hydrology, and contributions to current and future sea level rise require hydrological datasets to resolve. While direct observations of ice sheet meltwater losses can be obtained in terrestrial rivers draining the ice sheet and from lake levels, few such datasets exist. We present a new dataset of meltwater river discharge for the vicinity of Kangerlussuaq, Southwest Greenland. The dataset contains measurements of river water level and discharge for three sites along the Akuliarusiarsuup Kuua (Watson) River's northern tributary, with 30 min temporal resolution between June 2008 and August 2010. Additional data of water temperature, air pressure, and lake water level and temperature are also provided. Discharge data were measured at sites with near-ideal properties for such data collection. Regardless, high water bedload and turbulent flow introduce considerable uncertainty. These were constrained and quantified using statistical techniques, which revealed that the greatest discharge data uncertainties are associated with streambed elevation change and measurements. Large portions of stream channels deepened according to statistical tests, but poor precision of streambed depth measurements also added uncertainty. Data will periodically be extended, and are available in Open Access at doi:10.1594/PANGAEA.762818.

1 Introduction

Mean annual air temperatures over the Greenland ice sheet have warmed with 1.8 °C between 1840 and 2007 (Box et al., 2009). This trend has continued since 2007, with large surface air temperature anomalies along Greenland's coast in 2010 (Box et al., 2010). This observed warming is accompanied by a near-tripling of overall ice sheet mass balance losses since the 1960s (Rignot et al., 2008), with meltwater losses poorly constrained but estimated to be as much as twice the ice flow discharge losses between 2000 and 2008 (van den Broeke et al., 2009). Continued and increased mass

ESSDD
4, 71–97, 2011

A. K. Rennermalm et al.

losses from the Greenland ice sheet may have far reaching consequences, contributing perhaps 17–54 cm to global sea level rise by year 2100 (Table 3, line 3 in Pfeffer et al., 2008), while influencing regional meteorology (Dethloff et al., 2004) and ocean circulation in the North Atlantic (Driesschaert et al., 2007; Fichefet et al., 2003; Jungclaus et al., 2006). However, improved projections of future mass losses and their associated global and regional impacts require a better understanding of Greenland ice sheet hydrologic processes and runoff, especially proglacial river discharge which integrates runoff from the upstream ice sheet (Mernild and Hasholt, 2009; Rennermalm et al., 2011).

Where available, time-series of proglacial river discharge can reveal insights about englacial water storage dynamics (Mathews, 1963), meltwater travel time (Elliston, 1973), seasonal changes in subglacial drainage systems (when combined with dry tracer analysis, Nienow et al., 1998), supraglacial lake drainages and hydrologic drainage system (Bartholomew et al., 2011), and catastrophic drainage events in the proglacial environment (Mernild and Hasholt, 2009; Mernild et al., 2008; Russell et al., 2011). They are also valuable for estimating ice sheet meltwater losses, and have been extensively used for validation/calibration of ice sheet runoff models that extrapolate total meltwater losses for Greenland (Mernild et al., 2011) and elsewhere (Baker et al., 1982; Fountain and Tangborn, 1985; Hock and Noetzli, 1997; Klok et al., 2001; Verbunt et al., 2003). However, such measurements are rarely collected in Greenland, owing to inaccessibility and difficulties in measuring river discharge in gravel-bed braided river systems typical of proglacial environments (Ashmore and Sauks, 2006; Smith et al., 1996).

Here we present a new dataset (June 2008 to August 2010) of in situ hydrologic data collected at multiple proglacial sites in the upper Akuliarusiarsuup Kuua River drainage, Southwest Greenland. These include time-series of river water level recorded every 30 min, together with occasional in-channel measurements of flow width, depth, and velocity to retrieve discharge time-series from empirical rating curves constructed by relating water level to in situ discharge measurements. Other in situ measurements

ESSDD
4, 71–97, 2011

Proglacial river dataset from the Akuliarusiarsuup Kuua River

A. K. Rennermalm et al.

include lake water levels and temperatures, and barometric air pressure. Although, near-ideal sites were used to collect discharge measurements, strongly turbulent flows and high sediment bedloads in these proglacial rivers threatens to compromise data quality. Therefore, to build a higher-quality dataset, estimated uncertainties caused by changing streambed elevation, measurement errors, and rating curve fitting are also derived. Data are available in Open Access at doi:10.1594/PANGAEA.762818, and ongoing data collection will eventually allow extending the dataset further.

2 Site description

Three continuous river monitoring sites were selected along the Akuliarusiarsuup Kuua River's northern tributary (Sites 2, 3, and 4, Fig. 1, Table 1), with additional shorter period observations of a river and a lake (Sites 1, and 5, Fig. 1, Table 1). The Akuliarusiarsuup Kuua River is the northern branch of the Watson River that discharges into Kangerlussuaq Fjord near the town of Kangerlussuaq. All sites are located in the ice sheet proglacial zone, within 2 km of the ice edge and 27–30 km northeast of the town of Kangerlussuaq. Watersheds of Sites 3 and 4 are 7.8 and 64.2 km^2, respectively, and are both sub watersheds of Site 2's larger 101.4 km^2 watershed (Fig. 1 lower inset, delineated with ASTER GDEM, METI and NASA, accessed 2010). Meltwater runoff from the Greenland ice sheet is transported to these sites (2, 3, and 4) via different proglacial pathways, with varying degrees of upstream impoundment in lakes (Fig. 1). Prior to reaching Site 4, ice sheet meltwater is routed through one lake, whereas flows to Site 3 first pass through three to four upstream lakes. Site 2 integrates all water flow discharging from Lake A (Fig. 1), which includes flows from both Sites 3 and 4, plus a third inlet connecting Lake A and B at the southern side of the drainage basin. Upstream of this third inlet are two lakes, of which Lake C is usually ice dammed, causing meltwater to be routed to Lake B via an intermittent stream (Russell et al., 2011). More rarely, catastrophic drainage of the ice dammed Lake C occurs, as happened in 1987, 2007 and 2008 (Mernild and Hasholt, 2009; Mernild et al., 2008; Russell, 2009;

ESSDD
4, 71–97, 2011

Russell et al., 2011). When the ice dam burst, Lake C no longer drains via the intermittent stream, but discharges to Lake B from englacial/subglacial conduits along the ice margin (Russell et al., 2011).

3 Methods

River water level, temperature, and discharge measurements were collected at Sites 2, 3, and 4 (Table 1) between June 2008 and August 2010. Uncorrected river water level, $L_{\text{w-uc}}$, (Fig. 2) was determined as the difference between measured water pressure from submerged Solinst Levelogger pressure transducers (nominal precision 0.3 cm), and barometric air pressure recorded simultaneously with Solinst Barologger pressure transducers (nominal precision 0.1 cm) on land every 30 min. Leveloggers were enclosed in perforated steel boxes at the end of 1.5–3 m steel rods attached to bedrock or rocks, thus allowing direct emplacement in the stream without resting on the channel bed (Fig. 2, foreground). These boxes were maintained at a fixed depth relative to a datum plane and located within 1–30 m of the cross section used for in situ discharge measurements. Barologgers measuring air pressure were installed 150 m from Site 2 (Table 1) and assumed representative for all three gauging sites given the close proximity of these sites (less than 2 km) and the limited elevation differences between the sites. Data were retrieved from loggers in early June and late August of each year. From August to June Leveloggers were placed in rubber ballons filled with antifreeze solution to protect sensor from extreme pressures during freezing conditions (Solinst Inc., 2011). Regardless, some wintertime water level recordings at Site 2 displayed extreme pressure fluctuations probably due to freezing water, and were discarded from the dataset. Similarly, water temperature recordings at Site 2 were discarded from the dataset because they were controlled by interannual river ice thickness rather than stream water temperature. Data gaps during data downloading were filled by depth adjusting a secondary sensor to the main sensor. Estimated true water level at Levelogger installation sites, L_{w}, were calculated by adding $L_{\text{w-uc}}$ to the distance from logger steelbox to the stream bed, d_{box} (Fig. 2). Additionally, L_{w} time series were corrected

ESSDD
4, 71–97, 2011

for minor jumps in $L_{\text{w-uc}}$ time series due to slight differences in Levelogger placement in steel box following Levelogger retrieval for data downloading.

Discharge, Q, was determined at relatively stable river cross sections using the standard midsection method (WMO, 2010b), which requires collection of average velocity and water depth, d_{w}, at several measurement verticals in stream cross sections. These cross sections consisted of one incised bedrock channel (Site 2) and two structurally reinforced bridge crossings (Sites 3, and 4). Each cross section was marked at 1.0 m, 0.25 m, and 0.5 m intervals dividing cross sections into 21, 31, and 16 measurement verticals at Sites 2, 3, and 4, respectively, using bridges at Sites 3 and 4, and a suspended rope at Site 2 (Fig. 2, background). At each vertical, measurements of d_{w}, and velocity were collected using measurement rod/tape, and Price-type AA current meter. At Site 2, velocity measurements were made at 0.6 d_{w}, which typically equals average velocity along a vertical (e.g. WMO, 2010b). At Sites 3 and 4, velocity was measured at 0.1–0.3 m below the water surface, here stream flow was highly turbulent, shallow, and well mixed with a near-vertical velocity profile above the bed. Duplicate measurements conducted confirmed reproducibility of these near-surface velocity measurements at Sites 3 and 4. Thus, velocities determined at Sites 3 and 4 satisfy the measurement goals of determining average stream velocity for each vertical.

To assess changes in streambed elevation over time relative to a fixed point, cross sectional stream depths (d_{c}) were determined relative to a datum plane defined as the bottom edge of a steel beam supporting a bridge crossing the river (Sites 3, and 4) or the top of the iron rod installation (Site 2, Fig. 2). At Sites 3 and 4, d_{c}'s were measured from the bridges, simultaneous with d_{w}, and velocity measurements. At Site 2, physical separation of datum plane and stream cross section made simultaneous measurements impossible (Fig. 2). Instead, cross sectional stream depths were determined with a linear regression model constructed by relating occasional datum plane measurements to Solinst water depth recordings: $d_{\text{c}} = d_{\text{w}} + d_{\text{d}} - c_1 L_{\text{w}} - c_2$; where d_{c} is the cross sectional stream depth from datum plane, d_{w} is the cross section water depth, d_{d} is distance between datum and Solinst Levelogger enclosure, L_{w} is estimated distance

ESSDD
4, 71–97, 2011

Proglacial river dataset from the Akuliarusiarsuup Kuua River

A. K. Rennermalm et al.

between water surface and stream bed at Solinst Levelogger site. The coefficients c_1 and c_2 were determined through linear regression ($c_1 = 1.0$, $c_2 = 0.2$ m). Modeled and measured cross sectional stream depth correlated strongly ($r = 1.0$); hence, modeled d_c were used at Site 2.

Time-series of Q were retrieved from estimated true water level (L_w, determined as the sum of d_{box} and $L_{w\text{-uc}}$ measurements every 30 min corrected for jumps at data downloading, Fig. 2) via empirical rating curves constructed from occasional in situ measurements of Q. Empirical rating curves were derived by the typically used method of fitting first-degree power functions to in situ Q and ($L_w - d_0$) at corresponding times (e.g. WMO, 2010a), where d_0 is the water depth at zero discharge determined as minimum L_w (Site 2) or the lowest mode of L_w distribution (Sites 3 and 4). Defining d_0 as the lowest mode of L_w distribution effectively results in negative $L_w - d_0$ values, which can be interpreted as fluctuations cased by a noise in pressure measurements at times with no discharge. Thus, derived discharge was set to zero at subzero $L_w - d_0$ values. Power function best-fit parameters were determined using the linear least squares method. To fit the rating curve, 5, 17, and 16 discharge measurements were used for Sites 2, 3 and 4, respectively. To improve the Site 2 rating curve, a sixth point was added to represent peak conditions during the 31 August 2008 Jokulhlaup caused by drainage of the ice dammed lake (Lake C) by matching the recorded maximum L_w (470 cm) with an independent estimate of peak discharge (416 $m^3 s^{-1}$) from the ice dammed lake at that day (Russell et al., 2011). Indeed, calculated Jokulhluap volume (11.1×10^6 m^3) is similar to volume estimates based on detailed survey (12.9×10^6 m^3) (Russell et al., 2011).

In addition to pressure, Solinst Levelogger instrument records ambient water temperatures with a nominal precision of +0.05 °C. These temperature time-series are supplied for Sites 2, 3, and 4. A single year of lake water level and water temperature observations were collected at Site 5 (Table 1) between 2 June 2007 and 19 August 2008. Barometric pressure was collected at Site 1 between 2 June 2007 and 21 August 2009 (Table 1).

ESSDD
4, 71–97, 2011

Title Page
Abstract | Instruments
Data Provenance & Structure
Tables | Figures
◀| |▶
◀ ▶
Back | Close
Full Screen / Esc
Printer-friendly Version
Interactive Discussion

Discharge estimate uncertainty

Because of potential difficulties with making accurate and precise discharge estimates in high-bedload proglacial rivers (Ashmore and Sauks, 2006; Smith et al., 1996), hydrologic measurements from such environments must be carefully examined and their uncertainties quantified. Stability of d_c were examined by determining the slope of depth changes between June 2008 and August 2010 using linear regression analysis at each measurement vertical. Statistical significance of these slopes was determined with two-sided t-tests, at 0.1 significance level, testing the null hypothesis that these slopes were statistically similar to zero. Thus, rejecting the null hypothesis implies that d_c changed between June 2008 and August 2010. While establishing significance and magnitude of change, this trend analysis cannot provide insights into the cause of depth changes.

Two sources of flow depth error that propagate uncertainty to derived discharge estimates are temporal changes in bed elevation, which may increase or decrease the distance between the suspended pressure transducer and the channel floor (d_{box}); and human measurement error associated with d_w measurements in turbulent flow using steel rods and tapes. Owing to high bedload transport rates in the proglacial zone, changes in channel bed elevation are possible even in incised bedrock channels and at bridge crossings (Ashmore and Sauks, 2006; Smith et al., 1996), thus introducing irrevocable uncertainty to L_w time series derived from continuously recorded water surface elevation. Indeed, d_c observations were variable, both interannually and within a single field deployment. To examine the cause of this a one-way ANOVA analysis was employed.

This ANOVA analysis tested the null hypothesis that mean d_c at each vertical was statistically similar during all field deployments. Separate ANOVA tests were applied for each measurement vertical along the river cross section. Accepting the null hypothesis suggests that d_c's were statistically similar over time, which implies that observed temporal variability is due to measurement errors. This interpretation hinges on the

Discussion Paper | Discussion Paper | Discussion Paper | Discussion Paper |
ESSDD
4, 71–97, 2011
Proglacial river dataset from the Akuliarusiarsuup Kuua River
A. K. Rennermalm et al.

assumptions that depth variability within each field deployment reflects measurement uncertainty. This is a reasonable assumption given that field deployments were short (<7 days) and no major flooding occurred that could change streambed morphology. In theory, rejecting the null hypothesis would suggest that d_c's are changing between field seasons due to temporal changes in bed elevation. In practice, however, rejecting the null hypothesis could also reflect measurement uncertainty, particularly at Site 2 where different measurement tapes and sounding reels were used each year and where wind and stream flow conditions influenced the exact location of verticals. Additionally, strong stream flow positively bias d_w measurements made with reels and tape (WMO, 2010b). Thus, the ANOVA test outcome should be interpreted as follows: (1) accepting the null hypothesis provides strong evidence for measurement errors, (2) rejecting the null hypothesis is suggestive of bed elevation changes over time.

Discharge uncertainty was quantified by determining rating curves for upper and lower discharge ranges, Q_u and Q_l, respectively. The least-squares method was used to fit rating curve parameters to in situ discharge with added/subtracted maximum absolute deviation from mean stream velocity when duplicate measurements were available (Sites 3 and 4 only) and upper/lower boundaries of "true" water depth. "True" water depth boundaries were defined by the 90 % or greater confidence intervals of d_w measurements at each vertical. One of two methods was used to identify the "true" depth range depending on the outcome of the ANOVA test described above. If the null hypothesis was accepted at a 0.1 significance level, boundaries of true depth were determined as the 90 % confidence interval around d_c average using all field deployment data. If the null hypothesis was rejected, boundaries of true depth were determined as the maximum and minimum from upper and lower values of 90 % confidence intervals calculated separately for each deployment. Confidence intervals were determined using the t-distribution. In other words, this method produces narrower confidence intervals when the null hypothesis is accepted than when it is rejected, reflecting the greater certainty in streambed elevation when the hypothesis is accepted.

ESSDD
4, 71–97, 2011

4 Results

Even using "stable" channel cross sections, the surveyed d_c collected at Sites, 2, 3 and 4 show considerable variability and significant trends during five field deployments (June 2008, August 2008, June 2009, August 2009, and August 2010) (Fig. 3). Significant changes in d_c over time are found in 59 %, 45 %, and 13 % of measured verticals at 2, 3, and 4, respectively (Fig. 3, top panel). The majority of these trends reflect increasing channel depths over time. While the rate of channel deepening is generally slow at Sites 3 and 4 (average absolute change is 6 cm yr^{-1}), it can approach 50 cm yr^{-1} at Site 2 (Fig. 3, middle panel). Deployment average d_c vary, but observed temporal data ranges at a cross section measurement verticals can be as much as 3.2 m, 0.6 m, 1.4 m, at Sites 2, 3, and 4 (Fig. 3, lower panel).

This finding of changing streambed elevations over time reduces precision of derived discharge time-series and thus requires further quantification. A majority of measurement verticals along each stream cross section underwent changes in mean d_c between 2008 and 2010, verified by rejecting the null hypothesis of stable mean with a one-way ANOVA test (Fig. 4, top panels). By letting envelopes of true d_c vary according to the outcome of ANOVA tests (Fig. 4, bottom panels), unstable measurement verticals were given a greater range. Factoring in upper and lower ranges of true depth in calculations increases/decreases in situ discharge by an average of 14 %, 47 %, and 25 % of its value at Sites 2, 3 and 4, respectively. In comparison, the associated increase/decrease from factoring in velocity measurement deviation averages only 2 %, and 0 % of in situ discharge based on repeated measurements at Sites 3 and 4. The ANOVA test was rejected in 74 %, 71 %, and 56 % of measurement verticals along cross sections at Sites 2, 3, and 4. Had this test been rejected in the entire cross section, discharge uncertainties would have been much larger (on average 22 %, 66 %, and 36 % at Sites 2, 3, and 4) than if the test would have been accepted (on average 5 %, 11 %, and 7 % at Sites 2, 3, and 4). Thus, ANOVA test outcomes allow a better-constrained uncertainty estimates than if one of the two methods would have been used exclusively.

ESSDD
4, 71–97, 2011

Empirical rating curves relating time-series of $L_w - d_0$ to discharge were constructed using in situ discharge measurements from Sites spanning 2, 3, and 4 spanning 50 %, 45 %, and 65 % of observed above-zero $L_w - d_0$ data range, respectively (Fig. 5). These rating curves satisfactorily explain discharge variability (Table 2, associated with 99 %, 66 %, and 98 % of observed variance at Sites 2, 3 and 4). Most of $L_w - d_0$ laying outside the range covered by in situ discharge measurements occurred during winter low flow conditions, especially at Sites 3 and 4 where installed pressure transducers provided reliable data year-round. Only small fractions (0 %, 7 % and 2 % for Sites 2, 3 and 4, respectively) of observed water depths are greater than depths with the range covered by in situ discharge measurements. Thus, rating curves describe the bulk of warm season $L_w - d_0$ range adequately, including during high-flow conditions.

Stream discharge at all sites displays strong seasonal variability, and interannual variability that are robust within quantified uncertainty envelopes (Figs. 6, 7 and 8). Daily stream temperature variability is generally low, except during very low flow at Site 4 when the sensor was exposed between 22 August–2 September and 9 September–21 September in 2008, and between 6 September–4 October in 2009 (verified by comparing Levelogger temperatures with air temperatures). Some winter data retrievals for Site 2 were discarded, owing to implausible pressure variations, at sub zero temperatures, attributed to river ice processes (Fig. 6). Winter discharge retrievals for Site 3 and 4 include minor perturbations, and large discharge anomalies near the end of the year in 2008 and 2009 (only 2008 for Site 3). Discharge uncertainty is greatest at Site 3 (median uncertainty 69 % of observed values for the lower range, and 169 % of observed values for the upper range, Fig. 7). For Site 4, median lower and upper uncertainty ranges are 76 % and 123 %, respectively (Fig. 8). The lowest uncertainty is at Site 2, where median lower and upper uncertainty ranges are 91 % and 121 % (Fig. 6).

ESSDD
4, 71–97, 2011

Proglacial river dataset from the Akuliarusiarsuup Kuua River

A. K. Rennermalm et al.

5 Discussion

When proper procedure and equipment are used, discharge uncertainty largely stems from errors introduced during measurements of depth, width and velocity, and errors introduced by the water level-discharge relationship (Sauer and Meyer, 1992). A further complication is changing bed elevations over time, a phenomenon observed at all three of our discharge monitoring, particularly at Site 2. In situ discharge uncertainties due to depth errors associated with both measurements uncertainties and changing depth are large (14–47 %), while velocity uncertainties are small (0–2 %). Root mean square errors of rating curves are 2.0, 0.3, and 0.86 $m^3 s^{-1}$, which corresponds to 12 %, 17 %, 7 % of median discharge between day 166 and 227 (15 June–15 August in non-leap years) at Sites 2, 3, and 4, respectively (Table 2). Thus, errors associated with stream depth measurements and change propagate largest uncertainties to discharge retrievals.

Specialized techniques are needed to determine discharge during winter ice conditions (Pelletier, 1990; WMO, 2010a, 2010b). These techniques are not applied here because they require in situ measurements to be collected in winter, whereas all of our field deployments were in summer. However, while majority of discharge at subzero stream temperatures have been discarded for Site 2, they are retained in the database for Sites 3 and 4. Shallow stream depths at these two locations suggest that these streams are completely frozen during winter. During that time, L_w fluctuations can be considered background noise due to atmospheric conditions. Exceptions are two/one large L_w anomalies sustained for several days at Sites 3/4, exceeding background L_w noise, which suggest the possibility of occasional water discharge events at these sites even during winter; however further analysis is needed to confirm this. Because discharge retrievals from wintertime L_w fluctuations are highly uncertain, these data are provided as is without upper and lower data range constraints.

Flow depth uncertainties are associated with both ongoing temporal changes in streambed morphology and in situ measurement errors during field deployments. The

ESSDD
4, 71–97, 2011

latter is present across the entire width of the channel cross-section, and the former influences 74 %, 71 %, and 56 % of verticals in cross-sections of Sites 2, 3, and 4, respectively (Fig. 4). It is difficult to separate these two sources of depth uncertainty; however, streambed elevation measurements are positively biased during periods of strong flow suggesting that human measurement errors and drift in depth measurement devices may be a greater source of uncertainty than changing streambed elevations. Strong flows compromising in situ depth measurements were particularly pronounced during the 2010 field deployments at Site 2. Also, replicated depth measurements suggest that even small variations in horizontal position can result in large variations in vertical depth depending on the exact positioning of the rod end on abundant large cobbles (~0.2–1.0 m in diameter) present on the streambed.

Water level-discharge rating curves constructed using measurements during within-bank conditions become invalid during extreme floods, if flows overtop the riverbanks to spill into the surrounding floodplain. Although erosion marks suggest that this type of overflow has previously occurred at Site 2, all L_w's recorded during 2008–2010 were well below bankfull (~5–6 m). At Sites 3 and 4, the rating curve becomes invalid when flow overtops the bridge bottom. By identifying linear relationships between L_w and distance from bridge bottom to water surface at Sites 3 and 4, L_w of 140 cm and 120 cm, respectively, was found to coincide with the upper detectable limit of discharge. Such water levels were never exceed at Site 3, and only exceeded in 4 % of L_w observations at Site 4 during the study period.

6 Conclusions

Here, half-hourly hydrologic datasets of water level, temperature, and derived discharge are presented for proglacial streams and lakes draining the Greenland ice sheet near Kangerlussuaq. The dataset adds to a small collection of hydrologic datasets for Greenland, which are particularly rare for streams and rivers draining the ice sheet near its margin. Encountered limitations associated with turbulent water flow, high sediment bedloads, and ice were mitigated through quantitative error assessment. The resulting dataset is valuable for providing new insights into riverine conditions in the Southwest Greenland proglacial environment, the response of Greenland ice sheet meltwater runoff to climate variables, and possibly improved understanding of hydrologic processes operating within the ice sheet itself. Ongoing data collections at these sites are planned so that this dataset eventually can be extended further.

References

Ashmore, P. and Sauks, E.: Prediction of discharge from water surface width in a braided river with implications for at-a-station hydraulic geometry, Water Resour. Res., 42(3), W03406, doi:10.1029/2005WR003993, 2006.

Baker, D., Escher-Vetter, H., Moser, H., Oerter, H., and Reinwarth, O.: A glacier discharge model based on results from field studies of energy balance, water storage and flow, in: Hydrological Aspects of Alpine and High Mountain Areas (Proceedings of the Exeter Symposium, July 1982), 103–112, 1982.

Bartholomew, I., Nienow, P., Sole, A., Mair, D., Cowton, T., Palmer, S., and Wadham, J.: Supraglacial forcing of subglacial drainage in the ablation zone of the Greenland ice sheet, Geophys. Res. Lett., 38, L08502, doi:10.1029/2011GL047063, 2011.

Box, J. E., Yang, L., Bromwich, D., and Bai, L.: Greenland Ice Sheet Surface Air Temperature Variability: 1840–2007, J. Climate, 22(14), 4029–4049, doi:10.1175/2009JCLI2816.1, 2009.

Box, J. E., Cappelen, J., Decker, D., Fettweis, X., Mote, T. L., Tedesco, M., and Wal van de, R.: 2010 Greenland, In Arctic Report Card 2010, available at: www.arctic.noaa.gov/reportcard, 2010.

Dethloff, K., Dorn, W., Rinke, A., Fraedrich, K., Junge, M., Roeckner, E., Gayler, V., Cubasch, U., and Christensen, J. H.: The impact of Greenland's deglaciation on the Arctic circulation, Geophys. Res. Lett., 31, L19201, doi:10.1029/2004GL020714, 2004.

Driesschaert, E., Fichefet, T., Goosse, H., Huybrechts, P., Janssens, I., Mouchet, A., Munhoven, G., Brovkin, V., and Weber, S. L.: Modeling the influence of Greenland ice sheet melting on the Atlantic meridional overturning circulation during the next millennia, Geophys. Res. Lett., 34, L10707, doi:10.1029/2007GL029516, 2007.

ESSDD
4, 71–97, 2011

Elliston, G. R.: Water movement through the Gornergletscher, Int. Assoc. Sci. Hydrol., 95, 79–84, 1973.
Fichefet, T., Poncin, C., Goosse, H., Huybrechts, P., Janssens, I., and Treut, H. L.: Implications of changes in freshwater flux from the Greenland ice sheet for the climate of the 21st century, Geophys. Res. Lett., 30(17), 1911, doi:10.1029/2003GL017826, 2003.
Fountain, A. G. and Tangborn, W.: Overview of Contemporary Techniques, in: Techniques for Prediction of Runoff from Glacierized Areas, edited by: Young G. J., International Association of Hydrological Sciences (Red Book), 149, 27–41, 1985.
Hock, R. and Noetzli, C.: Areal melt and discharge modelling of Storglaciaren, Sweden, Ann. Glaciol., 24, 211–216, 1997.
Jungclaus, J. H., Haak, H., Esch, M., Roeckner, E., and Marotzke, J.: Will Greenland melting halt the thermohaline circulation?, Geophys. Res. Lett., 33, L17708, doi:10.1029/2006GL026815, 2006.
Klok, E. J., Jasper, K., Roelofsma, P., Gurtz., J., and Badouz, A.: Distributed hydrological modelling of a heavily glaciated Alpine river basin, Hydro. Sci.-J. Sci. Hydro., 46(4), 553–570, doi:10.1080/02626660109492850, 2001.
Mathews, W. H.: Discharge of a glacial stream, Int.Assoc. Hydrol. Sci., 63, 290–300, 1963.
Mernild, S. H. and Hasholt, B.: Observed runoff, jokulhlaups and suspended sediment load from the Greenland ice sheet at Kangerlussuaq, West Greenland, 2007 and 2008, J. Glaciol., 55, 855–858, doi:10.3189/002214309790152465, 2009.
Mernild, S. H., Hasholt, B., Kane, D. L., and Tidwell, A. C.: Jökulhlaup Observed at Greenland Ice Sheet, Eos Trans. AGU, 89(35), 321–322, doi:10.1029/2008EO350001, 2008.
Mernild, S., Liston, G., Hiemstra, C., Christensen, J., Stendel, M., and Hasholt, B.: Surface Mass Balance and Runoff Modeling Using HIRHAM4 RCM at Kangerlussuaq (Sondre Stromfjord), West Greenland, 1950–2080, J. Climate, 24(3), 609–623, doi:10.1175/2010JCLI3560.1, 2011.
METI and NASA: Japan's Ministry of Economy, Trade and Industry, METI, and National Aeronautics and Space Administration, NASA, available at: http://asterweb.jpl.nasa.gov/gdem.asp, 2010.
Nienow, P., Sharp, M., and Willis, I.: Seasonal changes in the morphology of the subglacial drainage system, Haut Glacier d'Arolla, Switzerland, Earth Surface Processes and Landforms, 23(9), 825–843, 1998.
Pelletier, P.: A review of techniques used by Canada and other Northern countries for mea-

Discussion Paper | Discussion Paper | Discussion Paper | Discussion Paper |

ESSDD
4, 71–97, 2011

Proglacial river dataset from the Akuliarusiarsuup Kuua River

A. K. Rennermalm et al.

surement and computation of streamflow under ice condtions, Nordic Hydrology, 21(4–5), 317–340, 1990.
Pfeffer, W., Harper, J., and O'Neel, S.: Kinematic constraints on glacier contributions to 21st-century sea-level rise, Science, 321(5894), 1340–1343, doi:10.1126/science.1159099, 2008.
Rennermalm, A. K., Smith, L. C., Chu, V. W., Forster, R. R., Box, J. E., and Hagedorn, B.: Controls on proglacial river discharge in Southwest Greenland, in preparation, 2011.
Rignot, E., Box, J., Burgess, E., and Hanna, E.: Mass balance of the Greenland ice sheet from 1958 to 2007, Geophys. Res. Lett., 35(20), L20502, doi:10.1029/2008GL035417, 2008.
Russell, A. J.: Jökulhlaup (ice-dammed lake outburst flood) impact within a valley-confined sandur subject to backwater conditions, Kangerlussuaq, West Greenland, Sediment. Geol., 215(1–4), 33–49, doi:10.1016/j.sedgeo.2008.06.011, 2009.
Russell, A. J., Carrivick, J. L., Ingeman-Nielsen, T., Yde, J. C., and Williams, M.: A new cycle of jökulhlaups at Russell Glacier, Kangerlussuaq, West Greenland, J. Glaciol., 57(202), 238–246, doi:10.3189/002214311796405997, 2011.
Sauer, V. and Meyer, R.: Determination of error in individual discharge measurments, USGS Open File Rep. No. 92-114, US Geological Survey, Norcross, Ga., 1992.
Smith, L., Isacks, B., Bloom, A., and Murray, A.: Estimation of discharge from three braided rivers using synthetic aperture radar satellite imagery: Potential application to ungaged basins, Water Resour. Res., 32(7), 2021–2034, 1996.
Solinst Inc.: Levelogger User guide Software 3.4.1, 16 January, 2011.
van den Broeke, M., Bamber, J., Ettema, J., Rignot, E., Schrama, E., van de Berg, W., van Meijgaard, E., Velicogna, I., and Wouters, B.: Partitioning Recent Greenland Mass Loss, Science, 326(5955), 984–986, doi:10.1126/science.1178176, 2009.
Verbunt, M., Gurtz, J., Jasper, K., Lang, H., Warmerdam, P., and Zappa, M.: The hydrological role of snow and glaciers in alpine river basins and their distributed modeling, J. Hydrol., 282(1–4), 36–55, doi:10.1016/S0022-1694(03)00251-8, 2003.
WMO: Manual on stream gauging – Computation of discharge, World Meterological Organization, ISBN 978-92-63-11044-2, 2010a.
WMO: Manual on stream gauging – Field methods, World Meterological Organization, ISBN 978-92-63-11044-2, 2010b.

ESSDD
4, 71–97, 2011

Table 1. Study sites and dataset variables. Dataset variables are: surface pressure (p_s), total pressure measured with solinst levelogger in stream, (p_t), water pressure (p_w), uncorrected water level (L_{w-uc}), water level (L_w), water temperature (T), discharge (Q), upper range of discharge (Q_u), and lower range of discharge (Q_l). Dataset also contain ags when dataset were augmented during data gaps.

Site	Full site name	Latitude	Longitude	Elevation (m)	Measured parameters	DOI
1	AK-001-001	67.078031	−50.276525	150	p_s	doi:10.1594/PANGAEA.762816
2	AK-002-001	67.132282	−50.138113	340	p_t, p_w, L_{w-uc}, L_w, T, Q, Q_u, Q_l	doi:10.1594/PANGAEA.762817
2	AK-002-002	67.131681	−50.137597	340	p_s	doi:10.1594/PANGAEA.762890
3	AK-003-001	67.143023	−50.122732	340	p_t, p_w, L_{w-uc}, L_w, T, Q, Q_u, Q_l	doi:10.1594/PANGAEA.762895
4	AK-004-001	67.146558	−50.106616	340	p_t, p_w, L_{w-uc}, L_w, T, Q, Q_u, Q_l	doi:10.1594/PANGAEA.762897
5	AK-005-001	67.149556	−50.125860	340	p_t, p_w, L_w	doi:10.1594/PANGAEA.762898

ESSDD
4, 71–97, 2011

Table 2. Model parameters and diagnostics for discharge rating curves. Rating curves are parameterized as rst degree power functions: $Q = C(L_w - d_0)^{\beta}$, where Q is discharge, C is a multiplier, L_w is water level at levelogger installation, d_0 is estimated water depth at zero discharge, and β is the exponent.

Site	C	β	R^2	RMSE	Datapoints
2	6.1×10^{-7}	3.4	0.99	2.0	7
3	6.5×10^{-5}	2.7	0.66	0.3	17
4	0.27	0.8716	0.81	0.81	16

ESSDD
4, 71–97, 2011

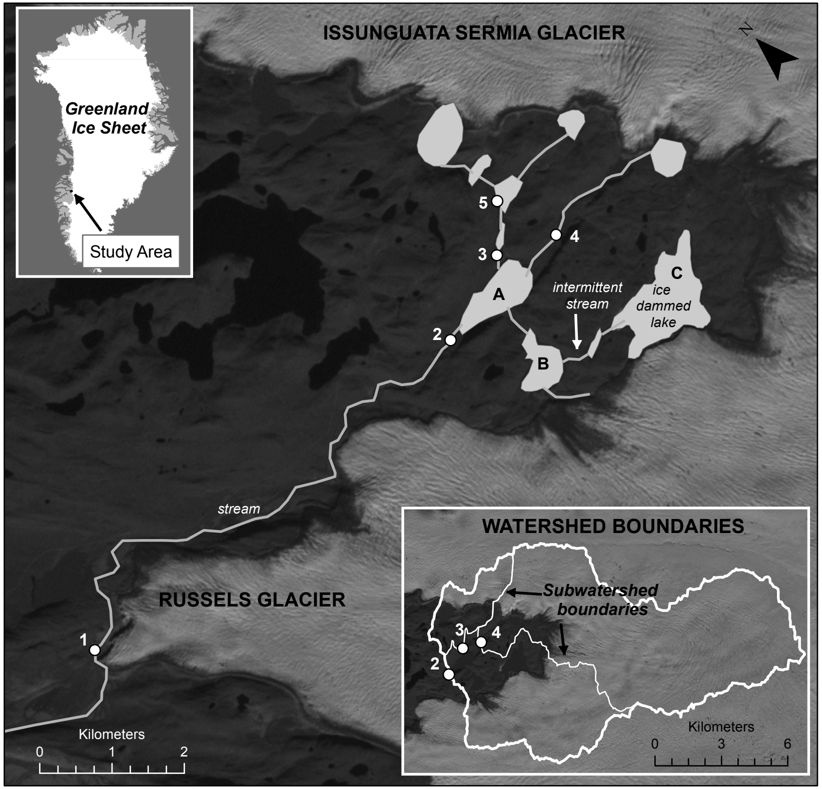

Fig. 1. Map of site locations in the proglacial environment, insets of Greenland map with study area (upper left corner), and inset of map with watershed boundaries upstream Sites 2, 3 and 4 (lower right corner). The Akuliarusiarsuup Kuua River's northern tributary, upstream proglacial lakes, streams, and monitoring sites (light gray) were manually digitized from a Landsat 7 ETM+ image from 23 August 2000 (also map background). Ice sheet appears white, land gray, and lakes are dark or grey.

ESSDD
4, 71–97, 2011

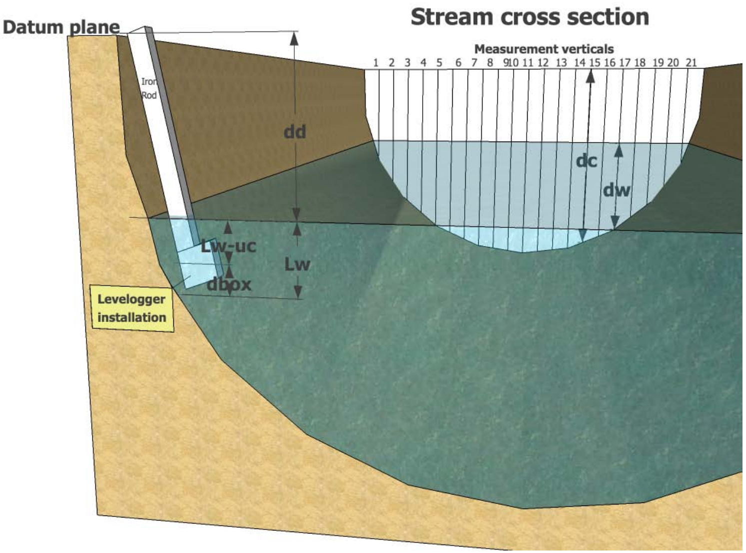

Fig. 2. Schematic figure showing installation at Site 2. A Solinst Levelogger is installed in a perforated steel box attached to an iron rod bolted to bedrock (foreground) where the top of the iron rod defines the datum plane. The distance from datum to Levelogger is denoted d_d, estimated true distance from stream bed to water surface, also referred to as water level, is denoted L_w, distance from Levelogger to streambed is denoted d_{box}, and uncorrected water level recorded by Leveloggers, $L_{w\text{-}uc}$, is distance from Levelogger to time varying water surface. Upstream of Levelogger installation (30 m) is the stream cross section where in situ discharge measurements are conducted using 21 measurement verticals (background). At each vertical, measurements are made of water depth (d_w) and stream velocity at 0.6 d_w. Distance from streambed to datum plane is also estimated for each vertical (d_c). Lengths of d_c and d_w are illustrated for interval 16 and 18 respectively, but are measured for all verticals 1 to 21. Installation setups at Sites 3 and 4 are the same, except that the datum plane is defined by a bridge, 31 or 16 verticals were used, and the Levelogger installation are in closer proximity (1–3 m) to measurement verticals.

ESSDD
4, 71–97, 2011

Proglacial river dataset from the Akuliarusiarsuup Kuua River

A. K. Rennermalm et al.

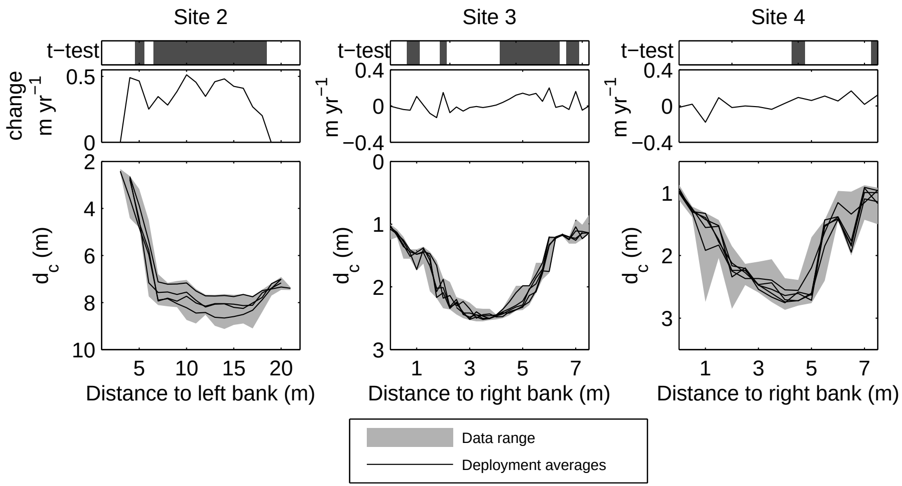

Fig. 3. Streambed elevation changes and measurement variability as a function of distance to left/right stream bank along cross sections. Top panels show outcome of t-test at each measurement vertical (gray shaded region indicate rejected null hypothesis of no streambed changes, and thus indicate significant change). Middle panels show streambed changes over time at each vertical in cross sections determined with linear regression model. Bottom panels show envelope of all d_c measurements (gray), and mean d_c in field deployments (black). The t-test was rejected in 59 %, 45 %, and 13 % of verticals at Sites 2, 3, and 4 suggesting that changing streambed elevation introduces uncertainty to derived discharge estimates.

ESSDD
4, 71–97, 2011

Proglacial river dataset from the Akuliarusiarsuup Kuua River

A. K. Rennermalm et al.

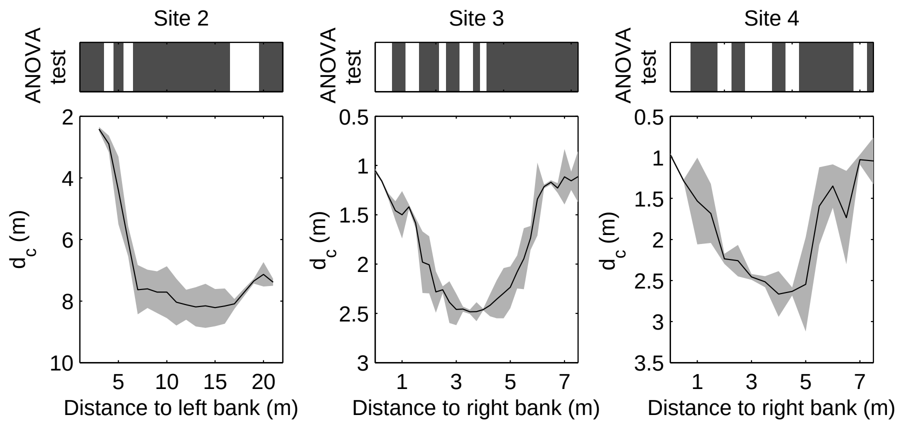

Fig. 4. Streambed elevation stability analysis with uncertainty envelopes of true d_c as a function of distance to left/right stream bank along cross sections. Top panels show outcome of one-way ANOVA testing stability of each measurement point along each stream cross section (gray shaded region indicate rejected null hypothesis, and thus an indicate unstable stream bed). Bottom panels show average d_c (solid black line), and the envelope between upper and lower range of true d_c (gray shaded). One-way ANOVA tests were rejected in majority of cross section lengths (74 %, 71 %, and 56 % at Sites 2, 3, and 4) suggesting changing streambed elevation here.

ESSDD
4, 71–97, 2011

Proglacial river dataset from the Akuliarusiarsuup Kuua River

A. K. Rennermalm et al.

Title Page
Abstract | Instruments
Data Provenance & Structure
Tables | Figures
◀| |▶
◀ ▶
Back | Close
Full Screen / Esc
Printer-friendly Version
Interactive Discussion

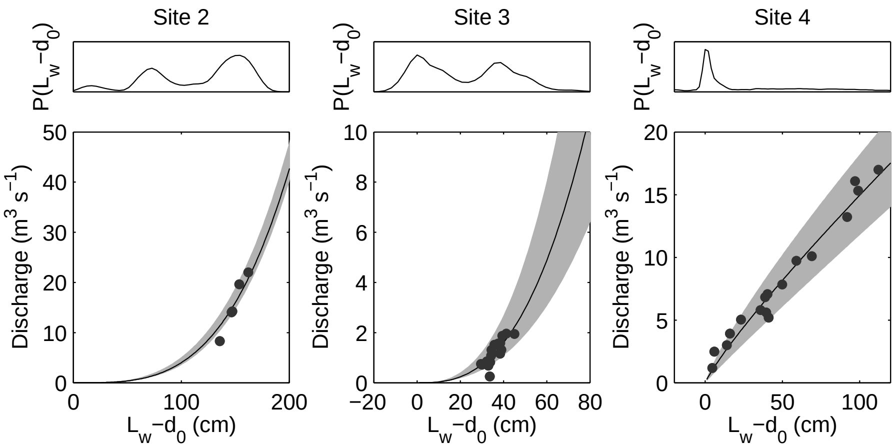

Fig. 5. Probability distribution of water levels ($L_w - d_0$) determined with kernel density functions (top panels). Discharge rating curves (solid black line), including observations (black points) and determined uncertainty range based on depth and velocity uncertainties (gray shaded) (bottom panels). The extreme discharge estimate at maximum $L_w - d_0$ observed at Site 2 on 31 August 2008 is not shown. $L_w - d_0$ associated with minimum and maximum in situ discharge observations contained 50 %, 45 %, and 65 % of observed above-zero $L_w - d_0$, and rating curves explained 99 %, 66 % and 98 % of in situ discharge variability at Sites 2, 3, and 4; rating curves and derived discharge can therefore be considered adequately representative of true conditions at these sites.

ESSDD
4, 71–97, 2011

Proglacial river dataset from the Akuliarusiarsuup Kuua River

A. K. Rennermalm et al.

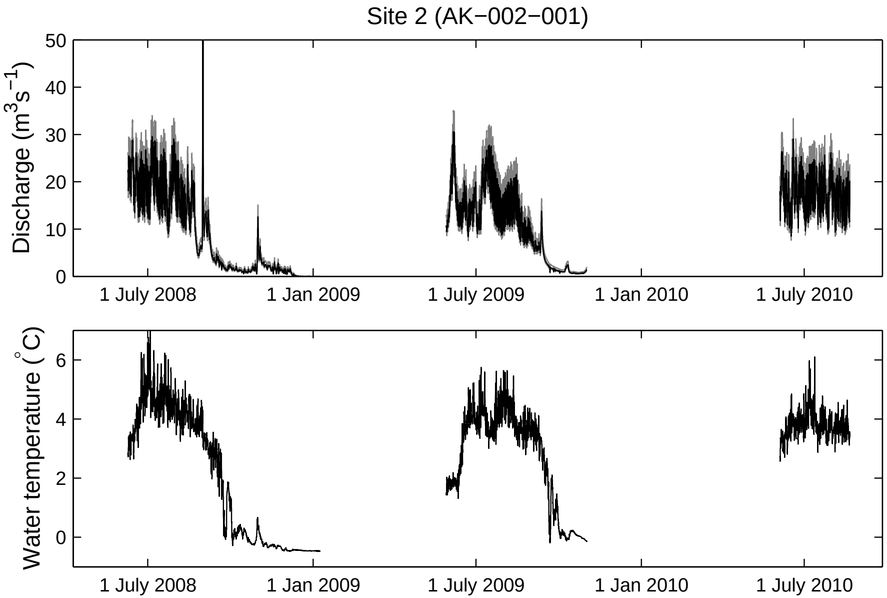

Fig. 6. Site 2 (AK-002-001) time-series of retrieved discharge and measured water temperature every 30 min (black lines). Upper and lower ranges of discharge retrievals are shown in grey. Majority of wintertime discharge was not calculated at Site 2 due to unrealistic Levelogger recordings at subzero temperatures at this site. Wintertime stream temperatures were also removed as they were controlled by interannual variability in river ice thickness rather than water temperatures.

ESSDD
4, 71–97, 2011

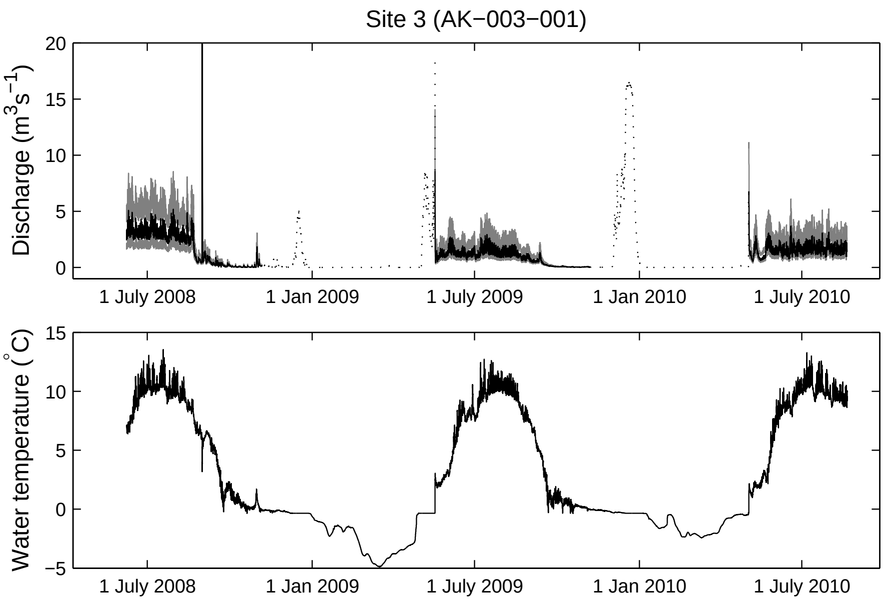

Fig. 7. Site 3 (AK-003-001) time-series, same as in Fig. 6. Wintertime (here defined as times with subzero stream temperatures) discharge uncertainty could not be constrained and are therefore not presented, and discharge values are stippled.

ESSDD
4, 71–97, 2011

Proglacial river dataset from the Akuliarusiarsuup Kuua River

A. K. Rennermalm et al.

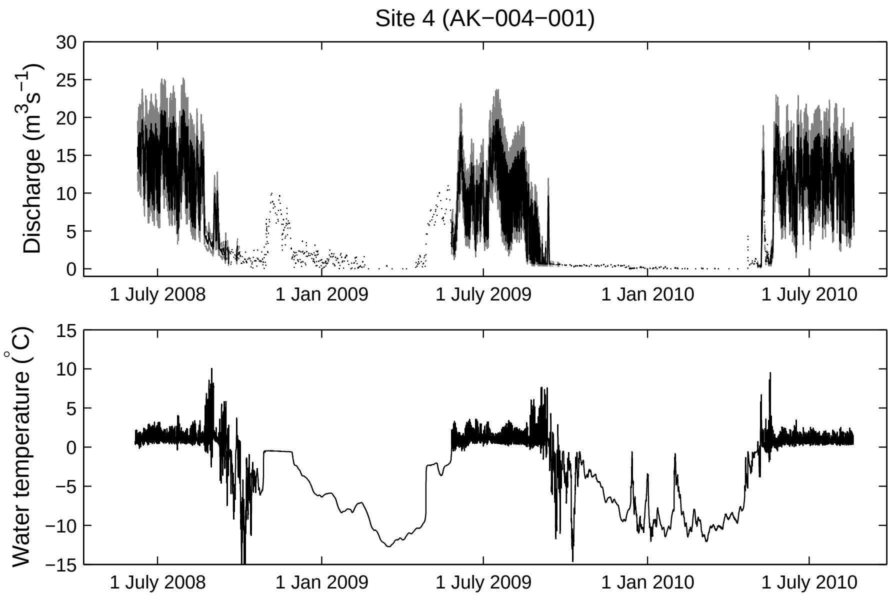

Fig. 8. Site 4 (AK-004-001) time-series, same as in Fig. 7.

ESSDD
4, 71–97, 2011